

Magnetic Compton scattering study of the Invar alloy Fe₃Pt

This article has been downloaded from IOPscience. Please scroll down to see the full text article.

1999 J. Phys.: Condens. Matter 11 L253

(<http://iopscience.iop.org/0953-8984/11/23/103>)

View [the table of contents for this issue](#), or go to the [journal homepage](#) for more

Download details:

IP Address: 171.66.16.214

The article was downloaded on 15/05/2010 at 11:46

Please note that [terms and conditions apply](#).

LETTER TO THE EDITOR

Magnetic Compton scattering study of the Invar alloy Fe₃Pt

George Srajer[†], C J Yahnke[†], D R Haeffner[†], D M Mills[†], L Assoufid[†],
B N Harmon[‡] and Z Zuo[‡]

[†] Advanced Photon Source, Argonne National Laboratory, Argonne, IL 60439, USA

[‡] Department of Physics and Astronomy, Iowa State University, and Ames Laboratory, USDOE,
Ames, IA 50011, USA

Received 6 May 1999

Abstract. The magnetic Compton profile (MCP) for ordered Fe₇₂Pt₂₈ has been measured at $T = 305$ and 490 K. The shape of the MCPs are compared to one obtained from first principles band-structure calculations for the ferromagnetic ground state. The theoretical analysis includes a decomposition of the various orbital and atomic contributions. The experiments indicate a discernible change in the shape of the MCP with increasing temperature, and possible implications for the observed change in shape are discussed.

Introduction

Beginning with Guillaume's pioneering work in 1896 [1], Invar alloys have been widely studied and used in numerous applications. From his initial work on the Fe–Ni alloy system, the term 'Invar' has been extended to include several other alloy systems, including Fe–Pt near the Fe₃Pt composition. As with the other Invar alloys, Fe₃Pt displays a small thermal expansion coefficient in a broad thermal range about room temperature. The mechanism responsible for this Invar effect, however, still remains the subject of debate [2–4]. While there have been many models proposed over the years (see [5–7] for relevant references), one of the earliest, the Weiss '2 γ -state model', has been widely used as a basis for analysis. Weiss postulated that γ -Fe (fcc) has two different, nearly degenerate, magnetic states [8]: γ_1 , a low spin (LS) state with a moment $\sim 0.5 \mu_B/\text{atom}$ and small atomic volume; and γ_2 , a high spin (HS) state with a moment $\sim 2.8 \mu_B/\text{atom}$ and a larger atomic volume. This model has been further developed and extended by several authors (Hillert [9], Bendick *et al* [10], and Matsui and Chikazumi [11]). In these models, the normal thermal expansion of the lattice is compensated by thermal excitation into the smaller volume γ_1 state. First principles calculations for fcc Fe as a function of volume have indeed shown energy minima for LS and HS states and have refined and increased the popularity of the two state concept [12]. More recent calculations [13, 14], which allow for noncollinear ordering of the magnetic moments, suggest that the LS state may in fact be due to more complicated magnetic orientation fluctuations than a simple local moment collapse.

Recently, experiments have been performed to test these theoretical calculations, but the results have proved inconclusive. Temperature-dependent photoemission experiments on Fe₃Pt have shown [5] a difference between the high and low temperature energy distribution curves for the collinear LS and HS states that are in reasonably good agreement with density of states calculations. Neutron scattering experiments made on Fe₃Pt in the paramagnetic temperature regime, on the other hand, have suggested that large local moments persist to

high temperatures [15]. It is our feeling that the LS state may indeed be some sort of noncollinear arrangement of fairly large local moments. However, the theory needed to establish such a model and obtain its thermal properties along with the magneto-lattice coupling is only now being developed [14]. Further experiments to ascertain details of the short-range magnetic order as a function of temperature are also needed. With this in mind, we have undertaken exploratory magnetic Compton profile (MCP) measurements on Fe₃Pt. To aid in the interpretation of the results and to investigate if the MCPs may be useful in providing information about the short-range magnetic order, we have performed corresponding first principles, spin-polarized band structure calculations for the ferromagnetic ground state of Fe₃Pt and obtained the theoretical MCP. Details of the experiments and calculations are given below.

Experimental details

Due to the inherently small cross section involved, magnetic Compton scattering (MCS) experiments have only become feasible with the advent of high energy synchrotron radiation sources. These experiments are still relatively new but are certain to become more commonplace with the arrival of high-brilliance third-generation storage rings. By alternately measuring the standard Compton profile with opposite sample magnetization (or photon helicity), MCS provides a measure of the momentum distribution of the difference between the spin-up and spin-down electrons. To be sensitive to the magnetic electrons, these experiments require circularly polarized photons that couple to the term in the incoherent scattering cross section arising from the interference between charge and magnetic scattering.

Compared to the charge scattering contribution, however, this term is down by a factor of $\hbar\omega/m_0c^2$, where m_0c^2 is the rest mass energy of the electron, and $\hbar\omega$ is the incident photon energy. Therefore, these experiments must be performed at relatively high photon energies in order to maximize the cross section for magnetic scattering. Operating at higher energies also simplifies the data analysis since it allows the scattering from the valence electrons to be treated within the impulse approximation [16] (i.e., far from any characteristic binding energies). With this approximation [17], the magnetic Compton cross section for a solid can be written [16–19] in a simple form given by:

$$\left[\frac{d^2\sigma}{d\Omega dp_z} \right]_{\uparrow} - \left[\frac{d^2\sigma}{d\Omega dp_z} \right]_{\downarrow} \equiv \left[\frac{d^2\sigma}{d\Omega dp_z} \right]_{\Delta} = P_c r_0^2 \left(\frac{k'^2}{k_0^2} \right) \Psi_2(\sigma) J^-(p_z) \quad (1)$$

where P_c is the degree of circular polarization, r_0 is the classical electron radius, and k_0 and k' are the magnitude of the incident and scattered x-ray wave vectors. Ψ_2 is a geometrical factor (see figure 1) defined as:

$$\Psi_2 = \pm\sigma (k_0 \cos \alpha \cos \varphi - k' \cos(\alpha - \varphi)) (\cos \varphi - 1) \frac{\hbar c}{m_0 c^2}. \quad (2)$$

Here, σ is the electron spin (± 1), α is the angle between the incident x-ray (\mathbf{k}_0) and the magnetic moment direction (\mathbf{B}), and φ is the scattering angle. The momentum distribution (p_z) of the unpaired electrons projected along the scattering vector, also known as the magnetic Compton profile, is contained in J^- (or J_{spin}):

$$J^-(p_z) = \iint (n^{\uparrow}(\mathbf{p}) - n^{\downarrow}(\mathbf{p})) dp_x dp_y \quad (3)$$

where the electron momentum density for a given spin orientation is given by $n^{\uparrow(\downarrow)}(\mathbf{p})$.

As seen from equations (1) and (2), the magnetic cross section for a given system (which is typically only 0.1% of the electronic charge cross section) can be increased by making the

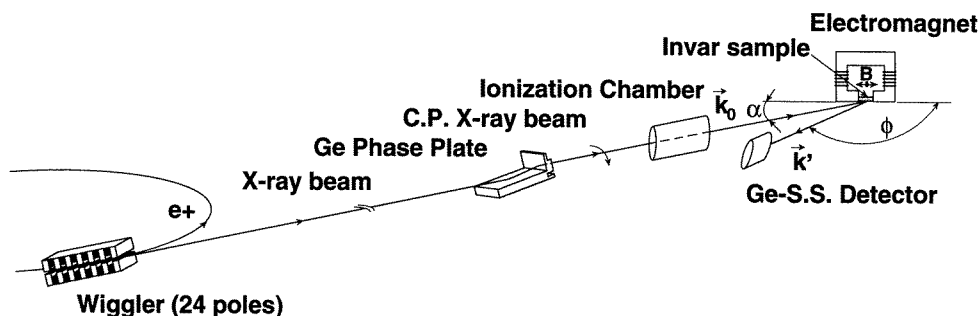


Figure 1. Schematic of the experimental setup. After the phase plate, the circularly polarized, monochromatic beam is incident on the sample placed between the poles of an electromagnet. The geometry is optimized to enhance the cross section as described in the text.

angle α smaller and ϕ larger. The first two factors are geometrical, and they were optimized for our particular experimental arrangement, as shown in figure 1.

Circularly polarized photons were obtained by employing a Bragg–Laue phase retarder constructed from single crystal germanium. This phase retarder operates at discrete energies within a range between 20–88 keV. The (440) crystal reflection produced a 90% degree of circular polarization for 65 keV x-rays used for this measurement. A detailed description of the phase retarder performance over its entire useful range is given elsewhere [20]. The photon energy of 65 keV was chosen for two reasons: one, it is sufficiently high enough for the impulse approximation to be valid; and two, it was the lowest incident energy whose broad Compton-shifted peak did not overlap with the Pt fluorescent K-edges.

Experiments were performed on the F2 wiggler beamline at the Cornell High Energy Synchrotron Source (CHESS). A 15 mm thick carbon filter and a 0.5 mm thick copper filter were used to remove the lower energy (220) harmonic reflection from the phase retarder and also to reduce the effects of heating caused by the wiggler white beam radiation. The 65 keV circularly polarized exit beam passed through a sealed Xe ion chamber, which acted as a beam monitor, before its incidence at 15° on the Fe_3Pt sample. The measured flux on the sample was 2.5×10^7 photons s^{-1} at 65 mA of storage ring current. This number was in a good agreement with the calculated flux. A scattering angle (ϕ) of 165° was chosen to maximize the magnetic Compton cross section within experimental constraints (figure 1). This produced a Compton shift of 13.15 keV with the inelastic peak centred about 51.85 keV.

The sample was prepared by arc melting Fe wire and Pt shot. It was then rolled into a $2 \times 2 \times 30$ mm ingot. The ordering of the sample was done in several steps. First, by heat treatment in vacuum at 650°C for 100 h, and then by gradual cooling to 450°C over 20 h. Subsequently, x-ray diffraction data were taken that confirmed the presence of the polycrystalline fcc Cu_3Au -like superstructure.

The sample was mounted in contact between the poles of an electromagnet with an applied field of 800 Gauss parallel to the sample face (figure 1). For the high temperature measurements, the sample was placed in a furnace with a built-in electromagnet. Contact between the sample and pole pieces was maintained throughout the experiment. The sample temperature was continuously held to within ± 3 K.

To distinguish the magnetic scattering from the charge scattering background, the measurements were made by obtaining data with opposite sample magnetizations, and the results were subtracted. The remaining profile is proportional only to the MCP. Alternatively, measurements can be made with elliptical (or circular) polarization of opposite helicity, with

the measured profiles subtracted as above. The former approach, however, is experimentally more practical, especially with soft, ferromagnetic samples. By constraining the sample magnetization and the incident and scattered wave vectors to be coplanar (figure 1), the measured profile depends only upon the scattering from the z -component of the electron's spin [21–23].

The data were collected using a Ge solid-state detector (Ge SSD) and a multichannel analyser in an ABBA sequence with one A or B step approximately 2 min long. At room temperature, 450 counts s^{-1} were obtained in the electronic Compton peak. To achieve acceptable statistical error, data were collected for the duration of 24 h. At high temperature (490 K), some of the lead shielding was removed around the Ge SSD so it was possible to move the detector closer to the sample to compensate for the anticipated loss in count rate due to the decrease in the sample's magnetization caused by the higher temperature. The closer proximity of the detector to the sample actually resulted in an increased counting rate in the electronic peak (1200 counts s^{-1}). Nevertheless, we collected data for the entire MCP over the 24 h period. The profiles were normalized relative to each other by counting versus a monitor (Xe ion chamber). The ordinate of the data has been transformed from energy to momentum in atomic units (a.u.) and folded about $p_z = 0$. An atomic unit of momentum (1.9929×10^{-24} kg m s^{-1}) is the momentum of an electron in the first Bohr orbit of hydrogen. The spacing between the points corresponds to the resolution of the Ge SSD (0.8 a.u.). The integral of the profile from -10 to $+10$ a.u. is directly proportional to the number of magnetic electrons or the magnetic moment/atom.

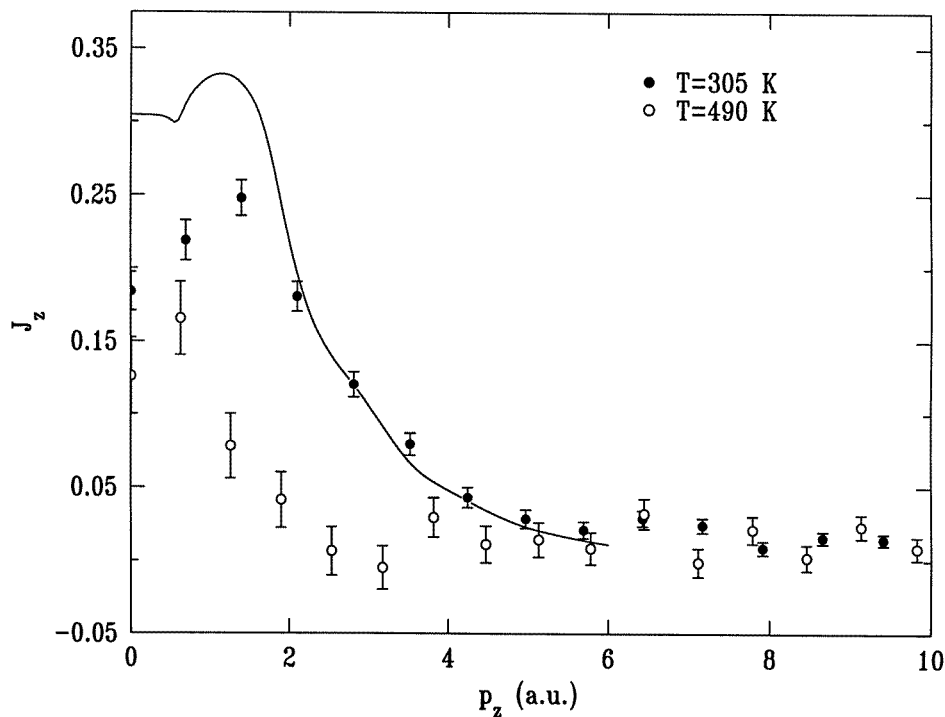


Figure 2. The experimental magnetic Compton profile (MCP) for ordered Fe_3Pt at 305 K (solid circles) and 490 K (open circles). The solid curve is the band theoretical MCP (see equation (3)), which has been normalized to yield the experimental value of the magnetic moment at 305 K.

As seen from figure 2, there is a significant difference in the shape of the profiles between the room and the high temperature data. In addition, both profiles have a maximum away from $p_z = 0$. The maximum and other features will be described in more detail below. The values of the moments were determined from the area of the measured profile, and normalized to a Fe standard with a known moment. The result for room temperature ($\mu = 1.8 \mu_B$) agrees well with previously published results [24].

Theoretical details

The self-consistent band structure calculations were performed using a spin-polarized, scalar relativistic version of the full potential linear-augmented plane wave (FLAPW) method. A mesh of 120 inequivalent k points in the irreducible Brillouin zone was used for the k -space integrations. We used the exchange-correlation potential of von Barth and Hedin as modified by Moruzzi *et al* [25]. The muffin-tin radii are 2.62 a.u. (1.38 Å) and 2.40 a.u. (1.27 Å) for Pt and Fe, respectively. With a lattice constant of 7.086 a.u. (3.75 Å) [26] the volume within the muffin-tin spheres is 70% of the total unit cell volume. The resulting band structure and density of states (DOS) are very similar to those obtained by Hasegawa using the APW method [27], and to those obtained by Podgórný using the LMTO method [12]. Table 1 contains a decomposition of the magnetic moments within each muffin-tin sphere. It is somewhat difficult to directly compare these values with those obtained by Podgórný because of the different partitioning of real space for the two methods. However, it seems our d-electron charge is more localized than his, and our net magnetic moment per cell of $8.21 \mu_B$ is larger than his value of $7.83 \mu_B$ (obtained at a smaller lattice constant, $a = 6.972$ a.u. = 3.689 Å). The Compton profiles were calculated for the ground state using a multi-atom per cell version of the method outlined by Wakoh and Kubo [28].

Table 1. The spin-up and spin-down charges for the various orbital components within the Fe and Pt muffin-tin spheres. The interstitial spin-up (spin-down) charge is 1.59 (1.63) with a net moment of $-0.04 \mu_B$. The d-orbital contribution is further broken down in e_g and t_{2g} components. The third row is the magnetic moment obtained by subtracting row two from row one.

	Total	s	p	d	d- e_g	d- t_{2g}	f	
Pt	4.79	0.33	0.20	4.22	1.72	2.50	0.03	
	4.44	0.36	0.25	3.80	1.54	2.27	0.02	
Fe	4.92	0.21	0.18	4.51	1.83	2.68	0.02	
	2.29	0.21	0.19	1.87	0.60	1.28	0.01	
Moment (μ_B)	Pt	0.35	-0.03	-0.05	0.42	0.18	0.23	0.01
	Fe	2.63	0.00	-0.01	2.64	1.23	1.40	0.01

Results

Figure 2 shows the experimental data for the ordered alloy taken at 305 and 490 K along with a theoretical profile. The theoretical curve is calculated for the ground state, $T = 0$ K, and was normalized to an area corresponding to an average moment per atom of $1.8 \mu_B$. This was done in order to facilitate comparison with the room temperature measurements. The area under the 490 K MCP curve corresponds to an average moment of $0.6 \mu_B$. All of the curves show a peak away from $p_z = 0$ and, while the curves are qualitatively similar in shape, it is the difference in shape that we wish to focus on. We begin by discussing the various contributions to the total MCP.

Figure 3 shows the MCP arising from the Fe 3d-orbitals, the Pt 5d-orbitals, and the total from these two d-contributions. When we refer to ‘orbital’ MCPs, we mean that we are taking the Fourier transform of the real-space wave function by restricting the integration over the muffin-tin sphere only, where the angular momentum character is well defined. In addition, figure 3 includes the curve giving the contribution from what we call the ‘interference’ term (explained further below) and the curve obtained from adding all the contributions to give the total MCP. The distinctive dip for small p_z in the total MCP curve, which causes it to fall below the d-orbital contribution, can be attributed to the negative polarization and the limited momentum range of the s and p valence electrons. Wakoh and Kubo [28] have previously pointed out the importance of the s and p negative polarization in producing a dip in the MCP of bcc Fe. The s and p orbitals are rather extended in real space and make up a significant part of the contributions to the MCP obtained by taking the Fourier transform of the spin density in the interstitial region between the muffin-tin spheres. The electronic wavefunctions in the interstitial region are expanded in plane waves, and we did not make an angular momentum decomposition for this region, since it would be approximate. The so-called interference term arises for many of the wavefunctions primarily because of hybridization between the more localized d orbitals and the extended s and p orbitals. To obtain the momentum density for a state, one must square the momentum wavefunction, which is just the sum of the Fourier transforms of the various components of the real space wavefunction. For wavefunctions with significant hybridization, the cross terms, particularly between the d-orbital Fourier transform

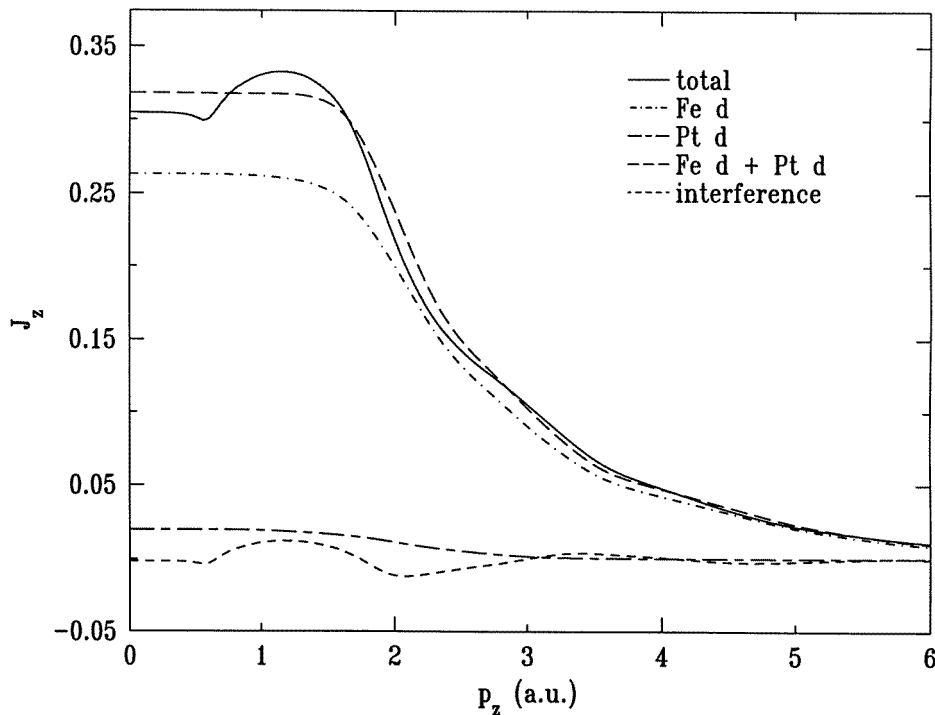


Figure 3. The theoretical MCP (solid curve) along with the contributions from the Fe d-orbital and Pt d-orbital moments (and their sum). The small oscillatory contribution shown arises from cross terms in the momentum profile having d-orbital contributions together with contributions from s, p, and interstitial parts of the wavefunction.

and the transform of the s-p contributions in the interstitial region, give rise to the interference term in the momentum density.

Conclusions

The experiments and calculations presented in this work were undertaken to determine if magnetic Compton scattering might provide some useful information concerning the temperature-dependent magnetic state of Fe₃Pt, an Invar alloy. The temperature-dependent data do indicate a change in the shape of the MCP between 305 and 490 K, where the 'Invar mechanism' is presumably active. The change in shape is rather dramatic and points to the desirability of a more systematic study of the progression of the MCPs starting at very low temperatures and extending into the paramagnetic region (where the net magnetization would be induced by applied fields).

We have used theoretical calculations to analyse the expected contributions to the $T = 0$ K ferromagnetic ground state MCP. Not surprisingly, the MCP is dominated by contributions from the Fe d-orbitals. However, the dip in the spectrum near $p_z = 0$ is associated with the small negative polarization of the s- and p-like electronic states. As these states are rather extended they dominate spin density in the interstitial region between the muffin-tin spheres. The s, p, and interstitial contributions to the momentum wavefunction and the d-orbital contributions produce an interference term when the momentum wavefunction is squared. This interference (cross term) and the explicit s and p terms in the momentum density are small compared to the d-orbital momentum density, but because they are negative and oscillatory their presence is easily detected. While small, we believe that these contributions may provide a means to analyse the temperature-dependent magnetic state. Since the s and p orbitals extend beyond a single site and 'sample' the environment (short-range order) of the surrounding d-moments, we believe the s, p, and interference MCPs could be useful for investigating the validity of different theoretical models. The problem is that the more recent theoretical models deal with complex magnetic orderings. To include temperature and noncollinear magnetic moment directions into calculations for such models necessitates dealing with the loss of periodicity (very large supercells with hundreds of atoms are required). Nevertheless there is a new theoretical method that has recently been proposed to deal with just such magnetic systems [14], and the implementation of the method on parallel computers has recently been achieved [29]. However, it will take some time to test the method before the calculation of the temperature-dependent MCP can be undertaken. In the meantime, we have performed a simple calculation to test if the shape of the MCP is at all sensitive to the magnetic state (to a first approximation one would expect that the MCP would simply scale with the average magnetization).

We have calculated the MCPs for Fe₃Fe (i.e., Fe has replaced Pt), for the ferromagnetic state and for a state with one of the Fe moments flipped (still collinear) giving rise to a ferrimagnetic arrangement. The two MCPs when normalized to the total magnetic moment per cell should have the same shape if the d-orbital contribution predominates. However, we find that the shape of the MCP corresponding to the ferrimagnetic state differs slightly from the MCP for the ferromagnetic state. In particular, it is about 5% smaller for $0 < p_z < 0.7$ and about 3% larger for $1.0 < p_z < 1.5$. These small differences are related to the extended s and p orbitals, and we expect precise measurements of the MCP can detect such effects. Thus it might be possible to use the s and p orbital contributions as a probe of the short-range magnetic order and how it changes as a function of temperature.

In conclusion, temperature-dependent MCS experiments on an ordered Fe₃Pt Invar alloy were performed. The results were analysed by self-consistent band-structure calculations

using a spin-polarized, scalar, relativistic version of the FLAPW method. The calculations confirmed the presence of the dip at $p_z = 0$ and that the shape of the profile is sensitive to the magnetic state. Future experiments are planned in which the counting statistics and the energy/momentum resolution will be substantially increased, and the temperature range will be extended.

The authors would like to thank E E Alp, J Quintana, and the entire staff at the Cornell High Energy Synchrotron Source for their help. They would also like to thank C Venkataraman and J Lang for helpful discussions. This work is supported by the US DOE-BES under contract no W-31-109-ENG-38. Part of this work was carried out at the Ames Laboratory, which is operated for the US Department of Energy by Iowa State University under contract no W-7405-82, and was supported by the Director of Energy Research, Office of Basic Energy Sciences of the US Department of Energy.

References

- [1] Guillaume C E 1896 *Compt. Rend.* **125** 235
- [2] Kisker E, Wassermann E F and Carbone C 1987 *Phys. Rev. Lett.* **58** 1784
- [3] Kakehashi Y 1988 *Phys. Rev. B* **38** 12 051
- [4] Bucholz B, Wassermann E F, Pepperhoff W and Acet M 1994 *J. Appl. Phys.* **75** 7012
- [5] Wassermann E F 1991 *J. Magn. Magn. Mater.* **100** 346
- [6] Wassermann E F 1989 *Phys. Scr. T* **25** 209
- [7] Wassermann E F 1987 *Festkörperprobleme Adv. Solid State Phys.* **27** 85
- [8] Weiss R J 1963 *Proc. Phys. Soc. London* **82** 281
- [9] Hillert M unpublished work discussed by Miodownik A P 1977 *CALPHAD* **1** 133
- [10] Bendick W, Ettwig H H, and Pepperhoff W 1979 *J. Magn. Magn. Mater.* **10** 214
- [11] Matsui M and Chikazumi S 1978 *J. Phys. Soc. Japan* **45** 458
- [12] Podgórný M 1991 *Phys. Rev. B* **43** 11300
- [13] Sandratskii I M and Guletskii P G 1986 *J. Phys. F: Met. Phys.* **16** L43
Sticht J, Höck K H and Kübler J 1989 *J. Phys.: Condens. Matter* **1** 8155
Uhl M, Sandratskii L M and Kübler J 1994 *Phys. Rev. B* **50** 291
- [14] Antropov V P, Katsnelson M I, van Schilfgaarde M and Harmon B N 1995 *Phys. Rev. Lett.* **75** 729
Antropov V P, Katsnelson M I, Harmon B N, van Schilfgaarde M and Kusnezov D 1996 *Phys. Rev. B* **54** 1019
- [15] Ziebeck K R A, Webster P J, Brown P J, Capellmann H 1983 *J. Magn. Magn. Mater.* **36** 151
Brown P J, Jassim I K, Neumann K U and Ziebeck K R A 1989 *Physica B* **161** 9
- [16] Platzman P and Tzoar N 1970 *Phys. Rev. B* **2** 3556
- [17] Sakai N and Ono K 1976 *Phys. Rev. Lett.* **37** 351
- [18] Cooper M J, Laundry D, Caldwell D A, Timms D N, Holt R S, and Clark G 1986 *Phys. Rev. B* **34** 5984
- [19] Mills D M 1987 *Phys. Rev. B* **36** 6178
- [20] Yahnke C J, Srajer G, Haeffner D R, Mills D M and Assoufid L 1994 *Nucl. Instrum. Methods* **347** 128
- [21] See, for example, Williams B (ed) 1977 *Compton Scattering* (New York: McGraw-Hill)
- [22] Cooper M J, Zukowski E, Collins S P, Timms D N, Itoh F and Sakurai H 1992 *J. Phys.: Condens. Matter* **4** L399
- [23] Timms D N *et al* 1993 *J. Phys. Soc. Japan* **62** 1716
- [24] Sumiyama K, Shiga M and Nakamura Y 1976 *J. Phys. Soc. Japan* **40** 996
- [25] Moruzzi V L, Janak J F and Williams A R 1978 *Calculated Electronic Properties of Metals* (New York: Pergamon)
- [26] We used the same lattice constant as Hasegawa [27], which is close to the value of 7.06 a.u. reported at 290 K by Sumayama K, Emoto Y, Shiga M and Nakamura Y 1981 *J. Phys. Soc. Japan* **50** 3296
- [27] Hasegawa A 1985 *J. Phys. Soc. Japan* **54** 1477
- [28] Wakoh S and Kubo Y 1977 *J. Magn. Magn. Mater.* **5** 202
- [29] Wang Y, Stocks G M, Nicholson D M C, Shelton W A, Antropov V P and Harmon B N 1997 *J. Appl. Phys.* **81** 3873